Supplementary Information for

Luminescent pentafluorophenyl-cycloplatinated complexes: synthesis, characterization, photophysics, cytotoxicity and cellular imaging

J. R. Berenguer,[a] J. G. Pichel,*[b] N. Giménez,[a] E. Lalinde,[a] M. T. Moreno,*[a] S. Piñeiro-Hermida.[b]

[a] *Departamento de Química-Centro de Síntesis Química de La Rioja, (CISQ), Universidad de La Rioja, 26006, Logroño, Spain.*

[b]*Centro de Investigación Biomédica de La Rioja (CIBIR), Fundación Rioja Salud, 26006, Logroño, Spain.*

Table of contents

Fig. S1 Selected region of the ^{1}H NMR spectra of Hbt, **1b**, **2b** and **3b** in CDCl$_3$ at 298 K
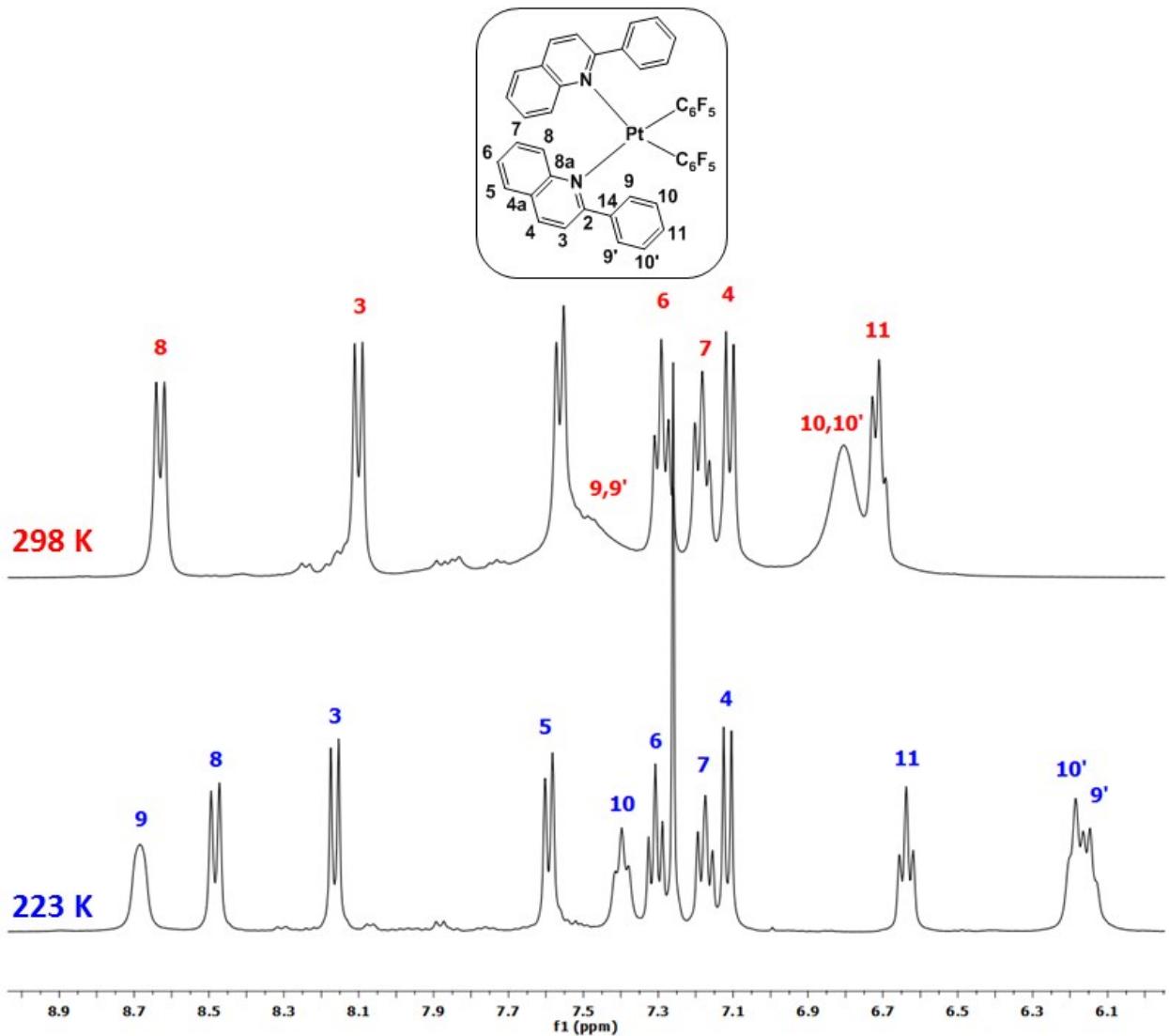
Fig. S2 ^{1}H NMR spectra of **1c** CDCl$_3$ at 298 K and at 223 K
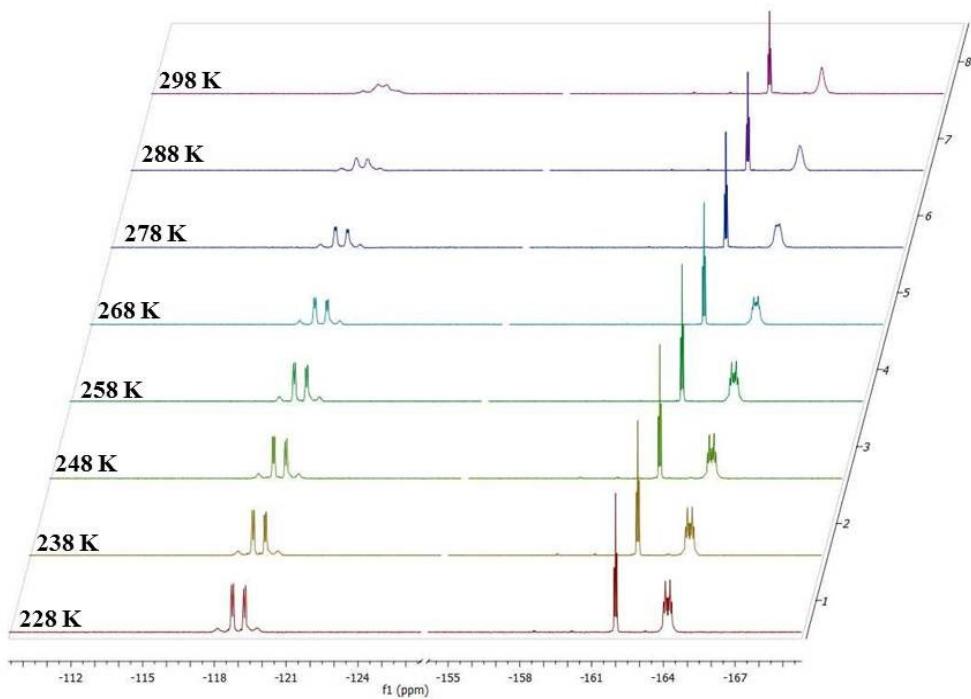
Fig. S3 Variable temperature ^{19}F NMR spectra of **1a** in CDCl$_3$
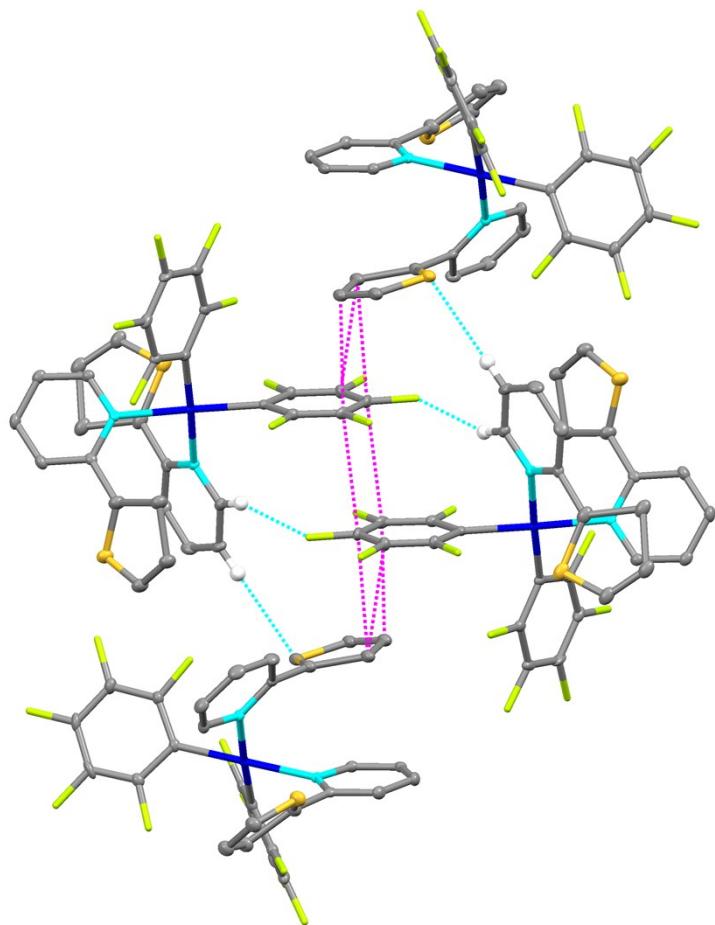
Fig. S4 Crystal packing of **1a** showing the intermolecular contacts. The supramolecular packing is formed by chains supported by intermolecular $\pi \cdots \pi$ (pink lines) involving Hthpy and C_6F_5 ligands with interplanar distances of 3.36 Å. These $\pi \cdots \pi$ interactions are supported by $F_{C6F5} \cdots H_{Hthpy}$ (2.38 Å) and $H_{Hthpy} \cdots S_{Hthpy}$ (2.86 Å) secondary interactions (blue lines).
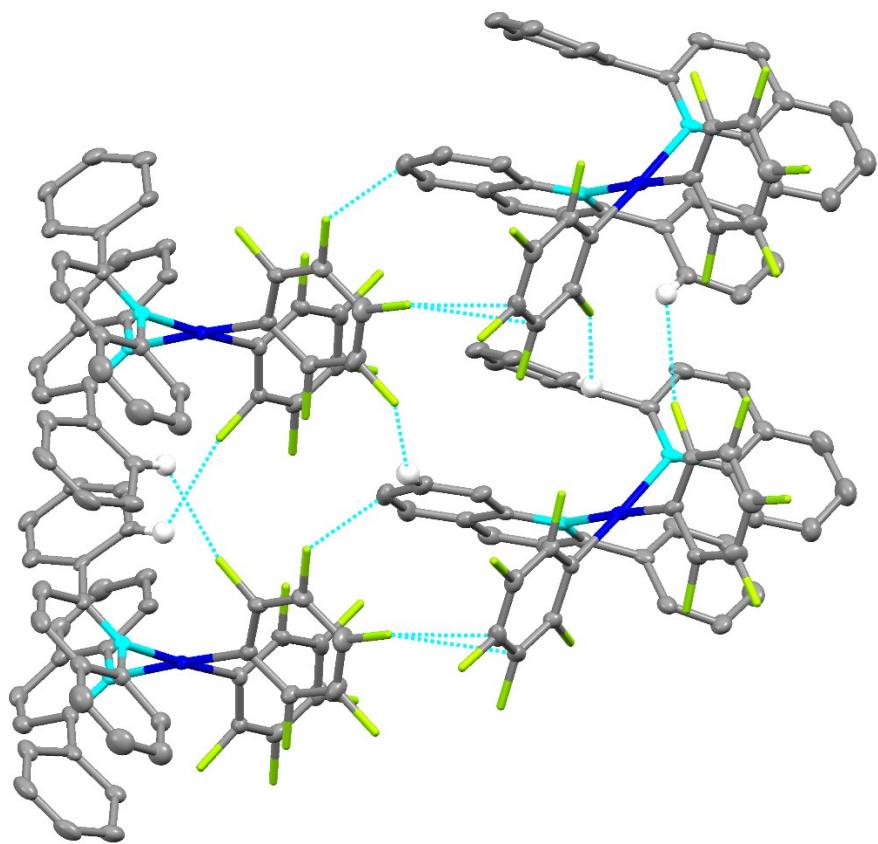
Fig. S5 View of the secondary interactions in the structure **1c**.0.75CH$_2$Cl$_2$. F$_{C6F5}$···C$_{C6F5}$ (3.04 Å), F$_{C6F5}$···C$_{Hpq}$ (3.15 Å) and F$_{C6F5}$···H$_{Hpq}$ (2.59 Å) interactions are observed.
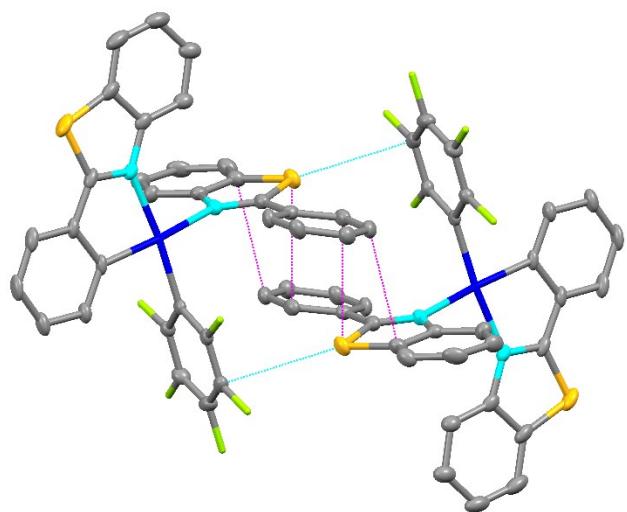
a)
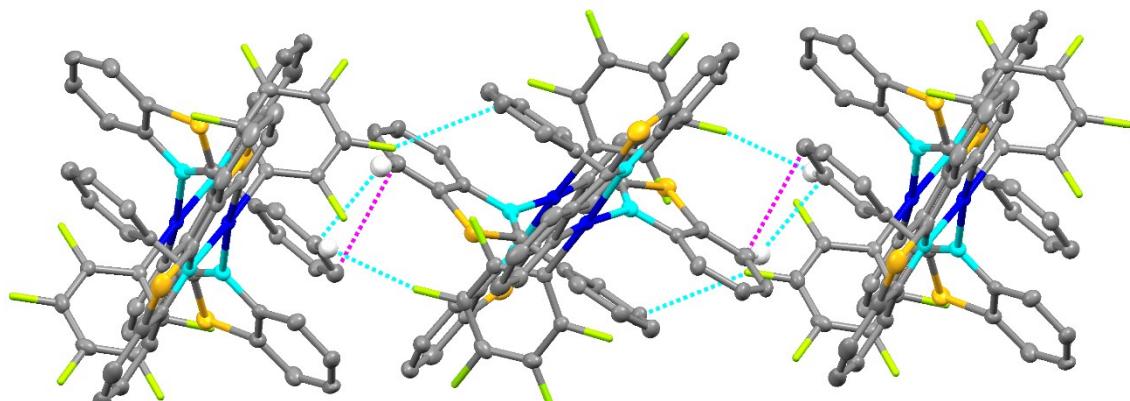
b)

Fig. S6 Crystal packing of the complex **2b** showing a) The supramolecular packing of the dimers supported by intermolecular $\pi\cdots\pi$ interactions (pink lines) involving Hbt ligands with interplanar distances of 3.31 Å ($C_{Hbt}\cdots C_{Hbt}$) and 3.50 Å ($S_{Hbt}\cdots C_{Hbt}$) supported by $C_{C6F5}\cdots S_{bt}$ (3.48 Å) secondary interactions (blue). b) The disposition of the chains sowing the interactions between dimers supported by $\pi\cdots\pi$ interactions ($C_{bt}\cdots C_{bt}$, 3.35, pink lines) and weak interactions (blue) [$H_{bt}\cdots F_{C6F5}$ (2.66 Å), $H_{bt}\cdots C_{bt}$ (2.81 Å), $C_{bt}\cdots F_{C6F5}$ (3.12 Å)]
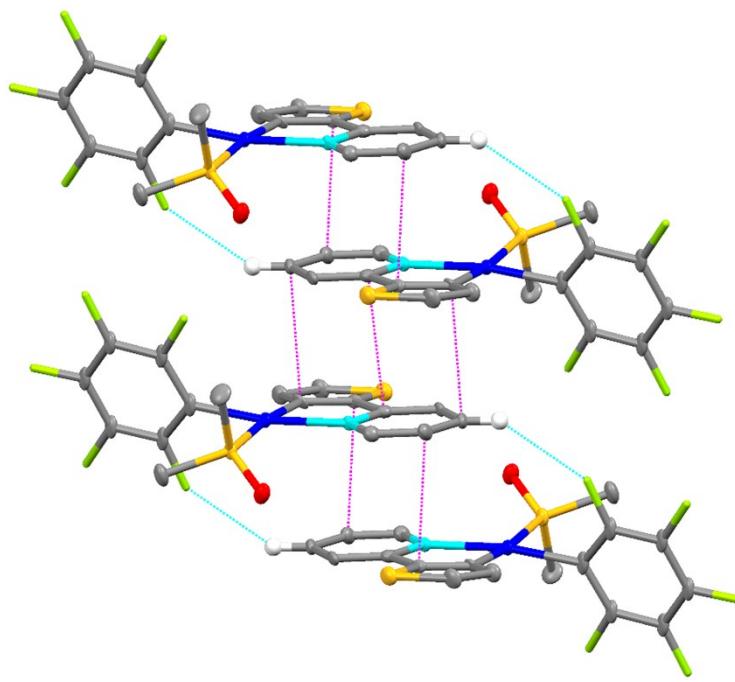
Fig. S7 Crystal packing of **3a** showing the intermolecular contacts. The supramolecular packing is formed by chains supported by intermolecular $\pi \cdots \pi$ (pink lines) involving two thpy ligands (3.33-3.40 Å). These $\pi \cdots \pi$ interactions are supported by $F_{C6F5} \cdots H_{thpy}$ (2.60 Å) (blue lines).
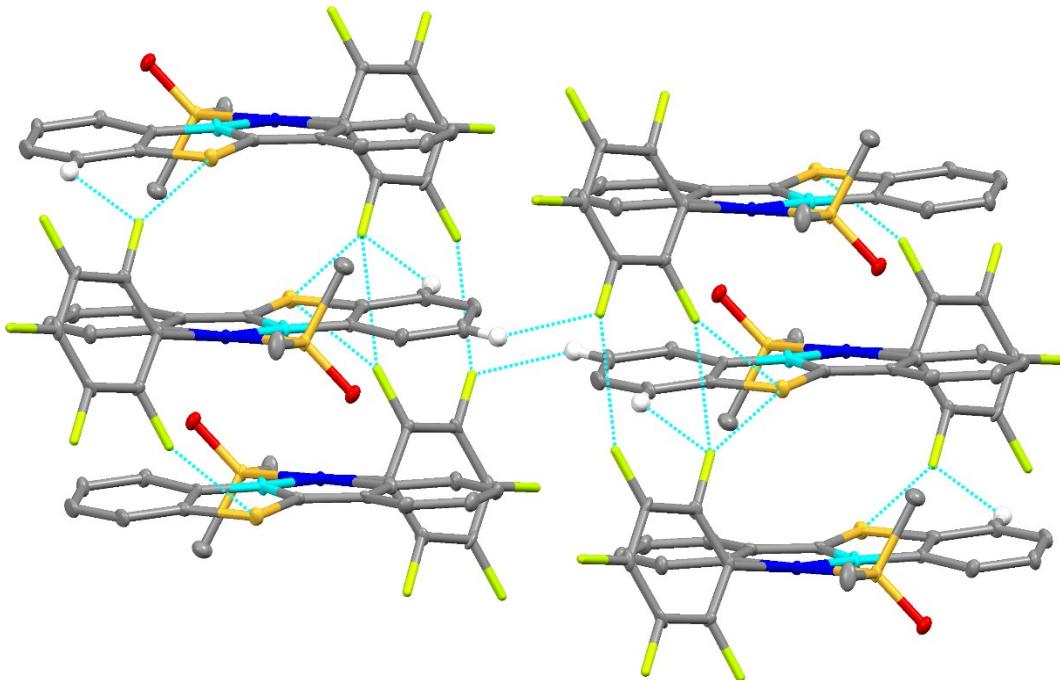
Fig. S8 View of the secondary interactions present in the structure **3b** showing the interactions $F_{C6F5} \cdots F_{C6F5}$ (2.84 Å), $F_{C6F5} \cdots H_{bt}$ (2.55-2.64 Å) and $F_{C6F5} \cdots S_{bt}$ (3.15-3.25 Å).
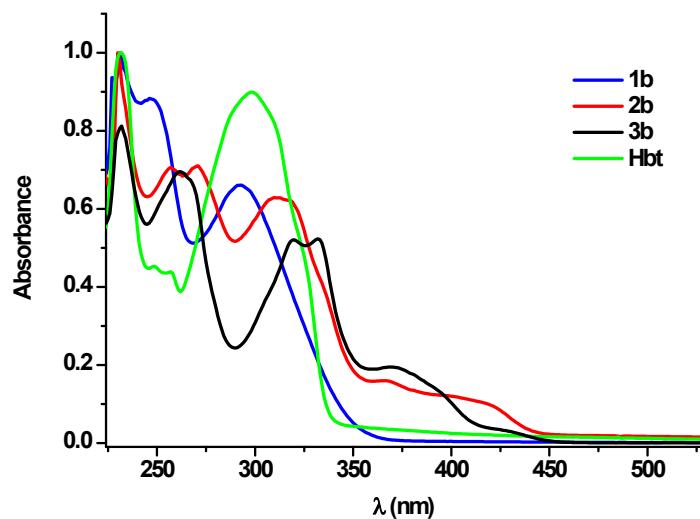
a)
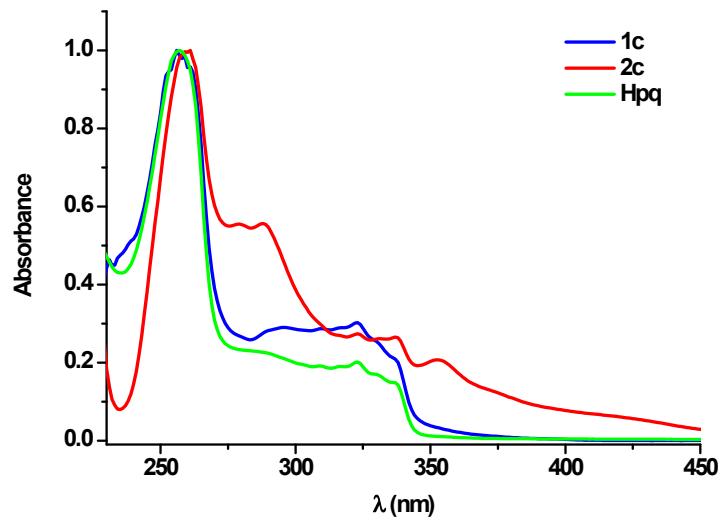
b)

Fig. S9. Absorption spectra in CH_2Cl_2 (5 x 10^{-5} M) at 298 K of a) the bt series of complexes (**1b**, **2b** and **3b**) and the Hbt ligand, b) the pq series of complexes (**1c** and **2c**) and the Hpq ligand
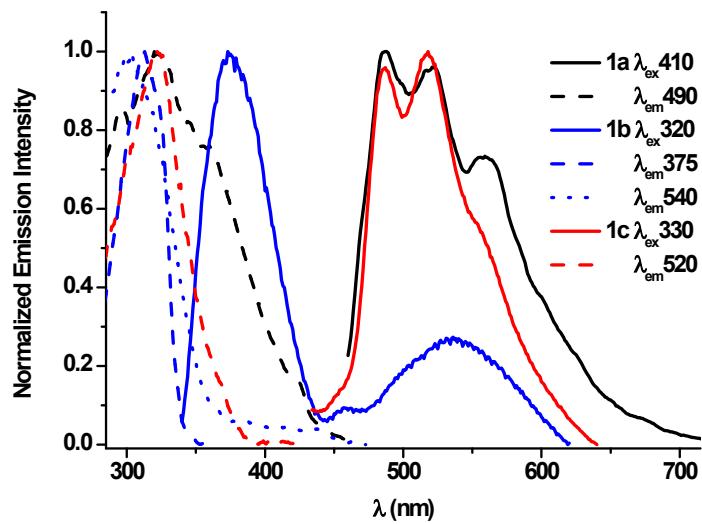
Fig. S10. Normalized excitation and emission spectra of **1a**, **1b** and **1c** in CH_2Cl_2 5 x 10^{-5} M at 298 K
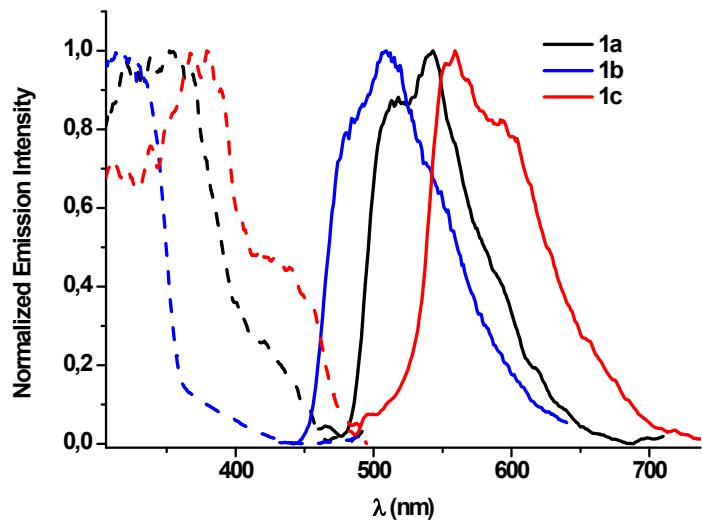
Fig. S11 Normalized excitation and emission spectra of **1a**, **1b** and **1c** in solid state at 77 K.
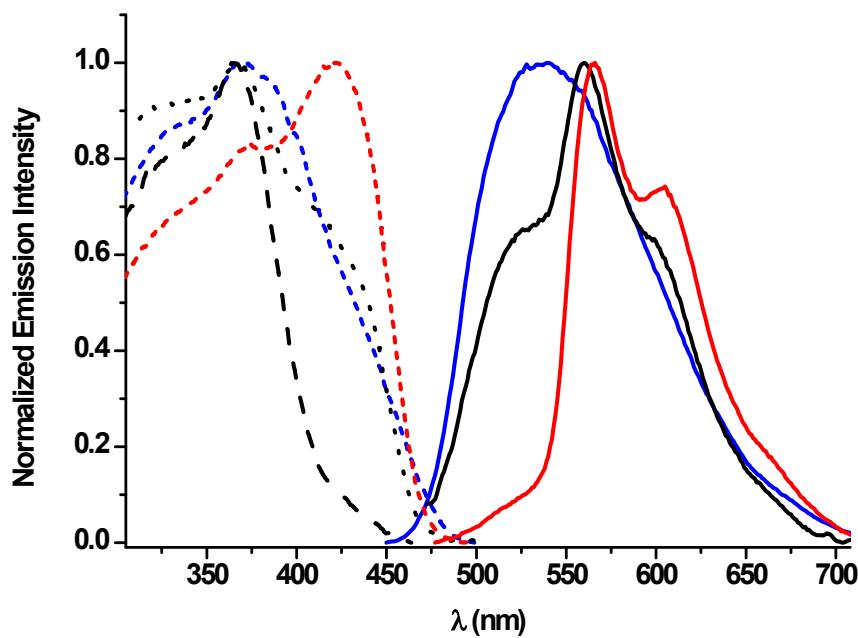
Fig. S12a Normalized excitation and emission spectra of different samples of **1a** in solid state at 298K: bulk material (black; the shape depends on the excitation wavelength), ground solid (red) and crystals obtained from CH_2Cl_2/n-hexane (blue) (λ_{exc} 365 nm)
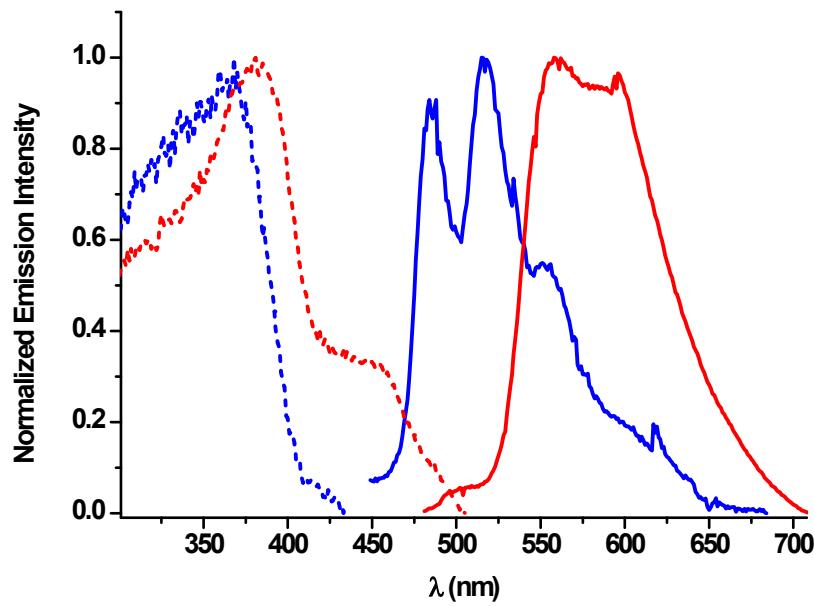
Fig. S12b Normalized excitation and emission spectra of different samples of **1c** in solid state at 298K: bulk material or ground solid (red) and crystals obtained from CH_2Cl_2/n-hexane (blue) (λ_{exc} 365 nm)
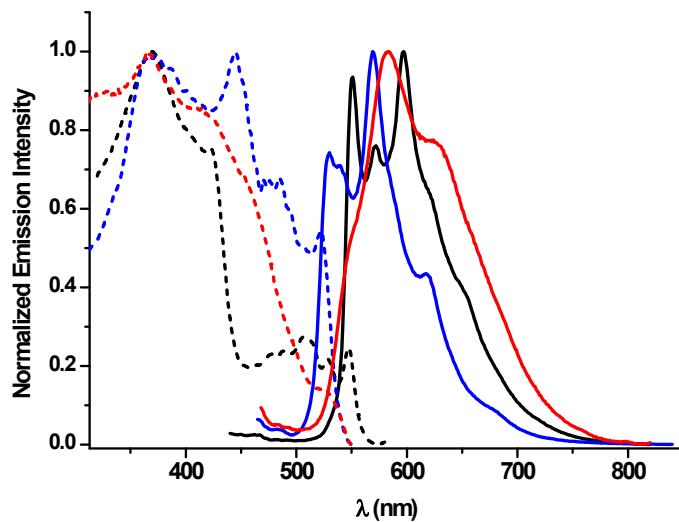
Fig. S13a Normalized excitation and emission spectra of **2a**, **2b** and **2c** in solid state at 298 K

Fig. S13b Normalized excitation and emission spectra of **2a**, **2b** and **2c** in solid state at 77 K.

Legend:
- 2a λ_{ex}365
- λ_{em}580
- 2b λ_{ex}365
- λ_{em}570
- 2c λ_{ex}365
- λ_{em}555
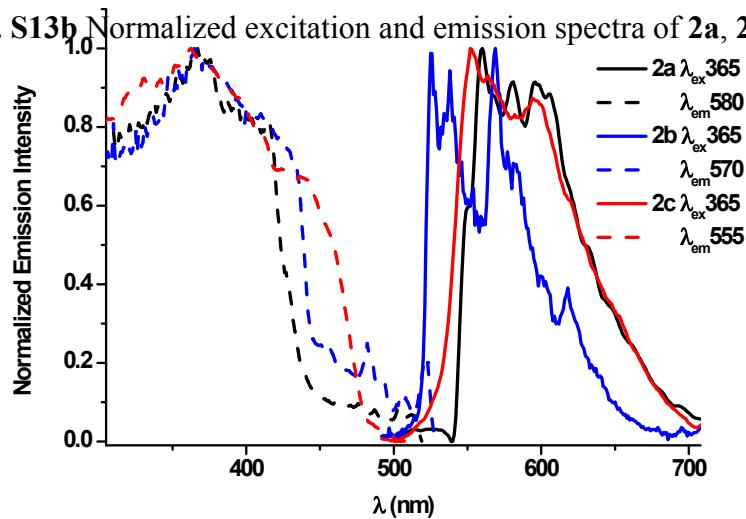
Fig. S14 excitation spectra of in CH$_2$Cl$_2$ 77 K.

Legend:
- 2a λ_{ex}410
- λ_{em}550
- 2b λ_{ex}365
- λ_{em}525
- 2c λ_{ex}420
- λ_{em}550
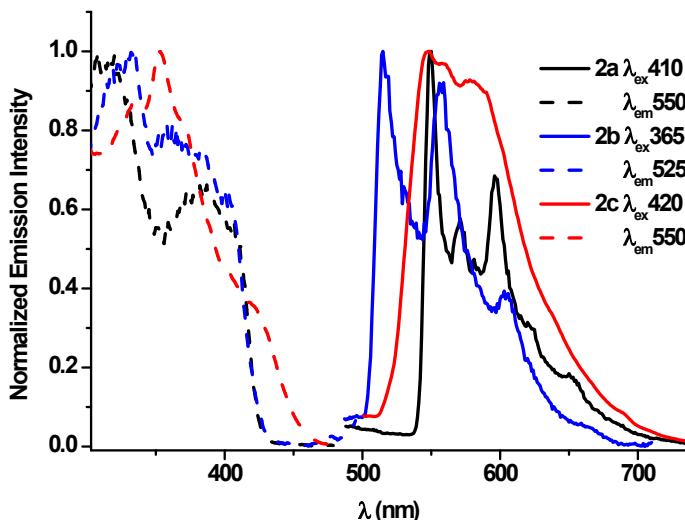
Normalized and emission **2a**, **2b** and **2c** 5 x 10^{-5} M at

S13
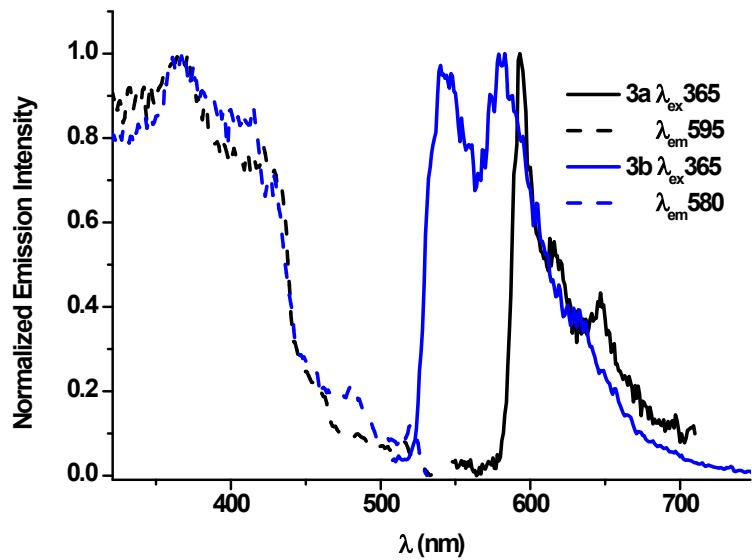
Fig. S15a Normalized excitation and emission spectra of **3a** and **3b** in solid state at 77 K
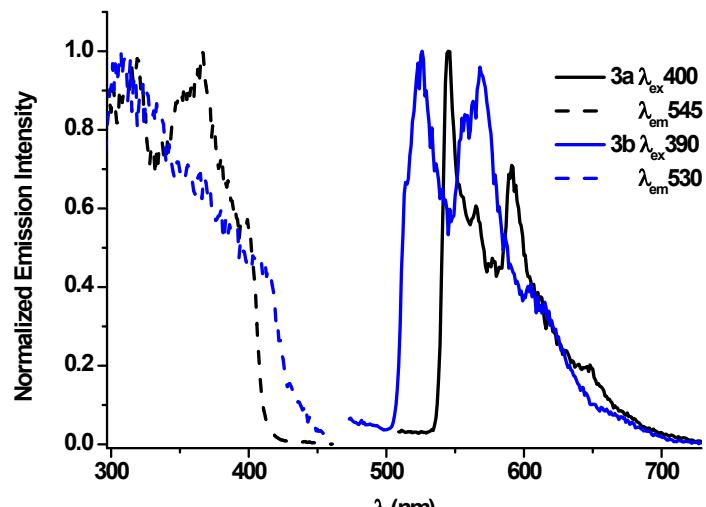
b)

Fig. S15b Normalized excitation and emission spectra of **3a** and **3b** in CH_2Cl_2 5×10^{-5} M at 77 K.

Table S1. DFT optimized geometries for ground state and triplet state of complexes **1a**, **1c 2b** and **3a**

1a			
	X-Ray	S_0	T_1
Pt-N(1)	2.110(3)	2.214	2.220
Pt-N(2)	2.111(3)	2.217	2.195
Pt-C(19)	2.012(4)	2.021	2.023
Pt-C(25)	2.015(4)	2.021	2.029
C(14)-C(15)	1.464(6)	1.469	1.393
Pt-H(16)	3.044	2.895	2.675
N(1)-Pt-N(2)	88.97(12)	89.65	88.62
C(19)-Pt-N(2)	88.80(14)	91.01	92.41
C(25)-Pt-N(1)	89.79(14)	91.88	91.77
C(19)-Pt-C(25)	92.46(16)	87.45	97.20

1c			
	X-Ray	S_0	T_1
Pt-N(1)	2.173(6)	2.251	2.163
Pt-N(2)	2.133(5)	2.251	2.254
Pt-C(31)	2.012(8)	2.030	2.047
Pt-C(37)	2.011(6)	2.030	2.023
Pt-H(14)	2.773	2.677	2.665
Pt-H(29)	2.759	2.677	2.710
N(2)-Pt-N(1)	90.1(2)	92.7	92.5
C(31)-Pt-N(2)	91.5(2)	90.9	90.0
C(31)-Pt-C(37)	87.2(3)	85.5	85.9
C(37)-Pt-N(1)	91.4(2)	90.9	91.5

2b			
	X-Ray	S_0	T_1
Pt-N(1)	2.101(3)	2.194	2.130
Pt-N(2)	2.152(3)	2.244	2.263
Pt-C(9)	2.007(3)	2.004	1.981
Pt-C(27)	2.005(4)	2.019	2.034
Pt-H(22)	2.587	2.831	2.890
Pt-H(15)	2.786	2.881	2.908

N(1)-Pt-N(2)	96.90(12)	99.14	98.61
C(27)-Pt-N(2)	90.65(12)	87.20	86.00
C(27)-Pt-C(9)	91.20(15)	93.72	93.36
C(9)-Pt-N(1)	81.37(15)	79.95	82.034

3a			
	X-Ray	S_0	T_1
Pt-N(1)	2.009(7)	2.168	2.139
Pt-C(1)	2.049(9)	2.005	1.975
Pt-S(2)	2.296(2)	2.438	2.450
Pt-C(10)	2.007(10)	2.034	2.041
O(1)-S(2)	1.472(6)	1.510	1.510
S(2)-C(16)	1.789(9)	1.819	1.820
S(2)-C(17)	1.795(9)	1.820	1.821
C(10)-Pt(1)-C(1)	91.5(4)	91.9	91.4
C(1)-Pt(1)-N(1)	79.0(3)	79.8	81.1
C(10)-Pt(1)-S(2)	92.0(3)	90.6	90.2
N(1)-Pt-S(2)	98.09(18)	97.8	97.4
O(1)-S(2)-Pt(1)	116.9(3)	120.1	120.4

1a	
S_0	T_1
1c	
S_0	T_1

2b	
S$_0$	**T$_1$**
3a	
S$_0$	**T$_1$**
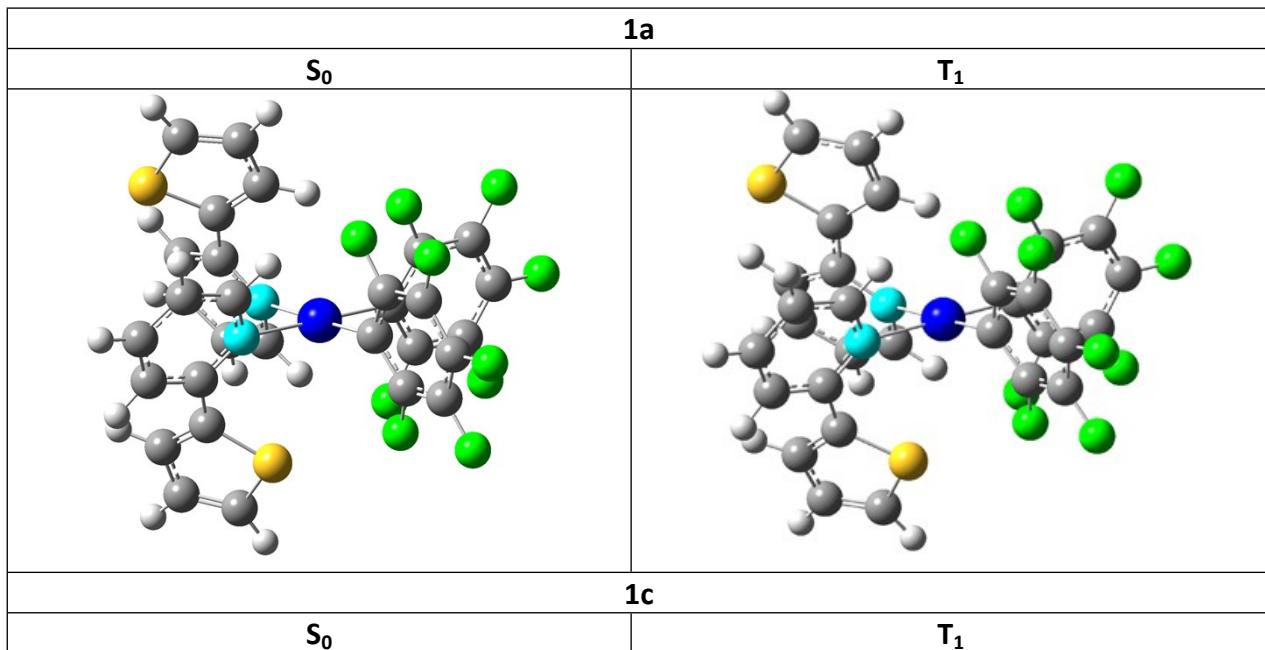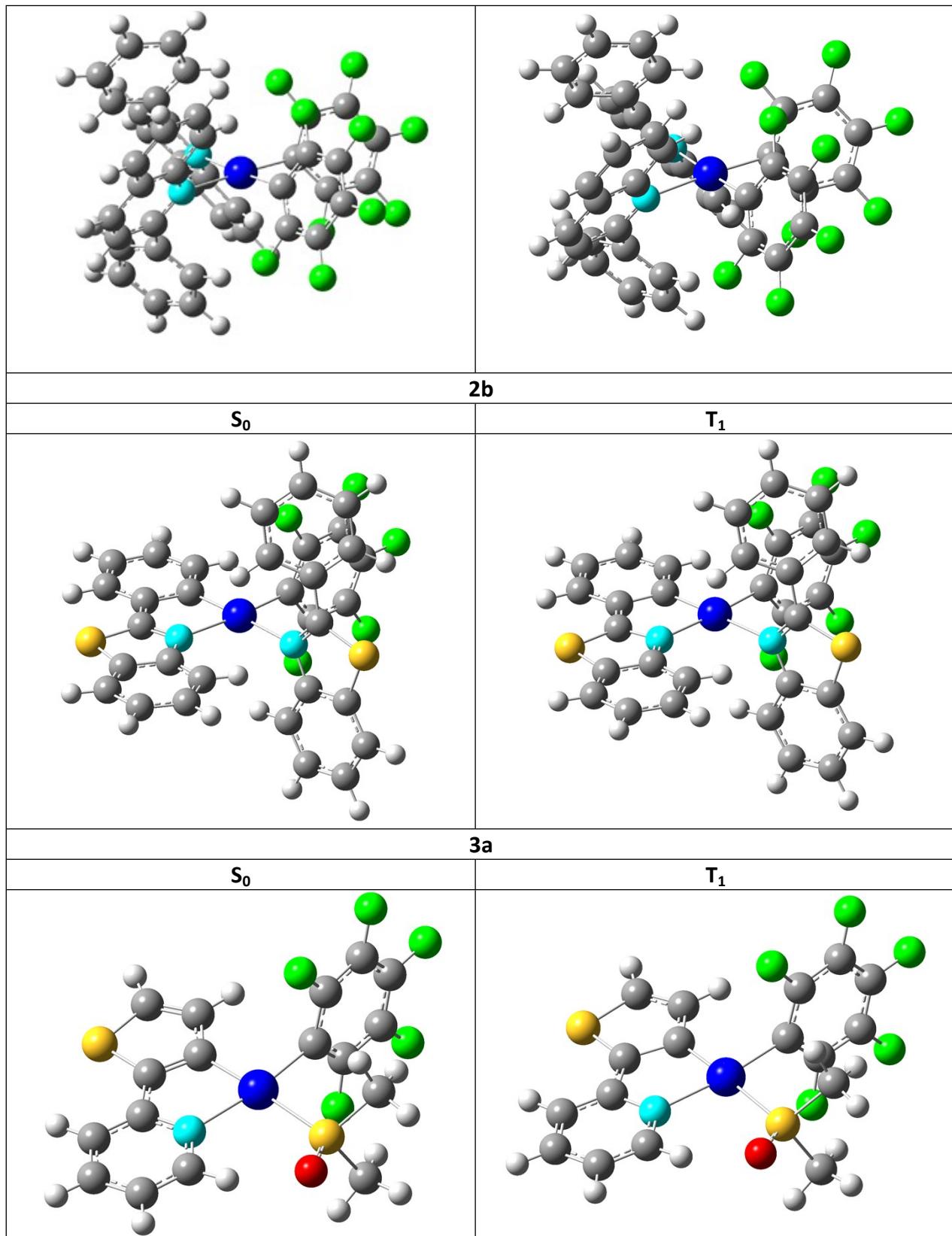
Fig. S16 Optimized structures of S$_0$ and T$_1$ states of **1a**, **1c**, **2b** and **3a**

Table S2 Composition (%) of Frontier MOs in the ground state for complexes **1a**, **1c**, **2b** and **3a** in gas phase.

		1a						**1c**				
MO	eV	C$_6$F$_5$(1)	C$_6$F$_5$(2)	Pt	Hthpy (1)	Hthpy (2)	eV	C$_6$F$_5$(1)	C$_6$F$_5$(2)	Pt	Hpq(1)	Hpq (2)
LUMO+5	-0.15	1	1	2	75	22	-0.3	2	2	2	49	45
LUMO+4	-0.52	24	25	34	10	8	-0.53	25	25	31	10	10
LUMO+3	-1.03	2	1	2	65	30	-0.81	1	1	1	49	48
LUMO+2	-1.18	0	1	1	31	67	-0.89	0	0	1	49	50
LUMO+1	-1.66	0	0	2	72	26	-1.92	0	0	1	49	49
LUMO	-1.74	0	0	1	27	72	-2.02	0	0	1	49	49
HOMO	-5.82	3	3	73	10	11	-5.86	4	4	82	5	5
HOMO-1	-6.02	34	31	32	2	1	-6.01	28	28	30	7	7
HOMO-2	-6.23	17	19	33	14	17	-6.15	26	26	30	9	9
HOMO-3	-6.39	18	1	16	45	21	-6.37	46	49	3	1	1
HOMO-4	-6.39	41	45	3	4	7	-6.38	6	4	39	26	26
HOMO-5	-6.46	41	52	1	5	1	-6.48	48	47	4	1	1

		2b					**3a**			
	eV	bt	Hbt	C$_6$F$_5$	Pt	eV	C$_6$F$_5$	thpy	dmso	Pt
LUMO+5	-0.3	21	45	16	13	0.1	31	11	27	30
LUMO+4	-0.43	37	57	2	4	0.03	82	5	1	11
LUMO+3	-0.52	51	47	0	2	0.01	65	7	15	13
LUMO+2	-0.61	15	77	2	5	-0.6	33	24	11	32
LUMO+1	-1.91	4	94	0	1	-1.05	0	98	0	1
LUMO	-1.94	91	5	0	4	-1.84	1	89	2	8
HOMO	-5.82	63	1	0	35	-5.74	0	85	1	14
HOMO-1	-5.97	4	5	4	87	-6.33	68	5	3	25
HOMO-2	-6.12	3	3	66	28	-6.41	15	4	0	81
HOMO-3	-6.32	58	1	3	38	-6.46	50	42	0	7
HOMO-4	-6.39	1	1	99	0	-6.51	49	41	0	10
HOMO-5	-6.53	69	9	2	20	-6.92	4	14	0	81

LUMO +1   LUMO +2   LUMO +3

HOMO   LUMO

HOMO -1   HOMO -2   HOMO -3
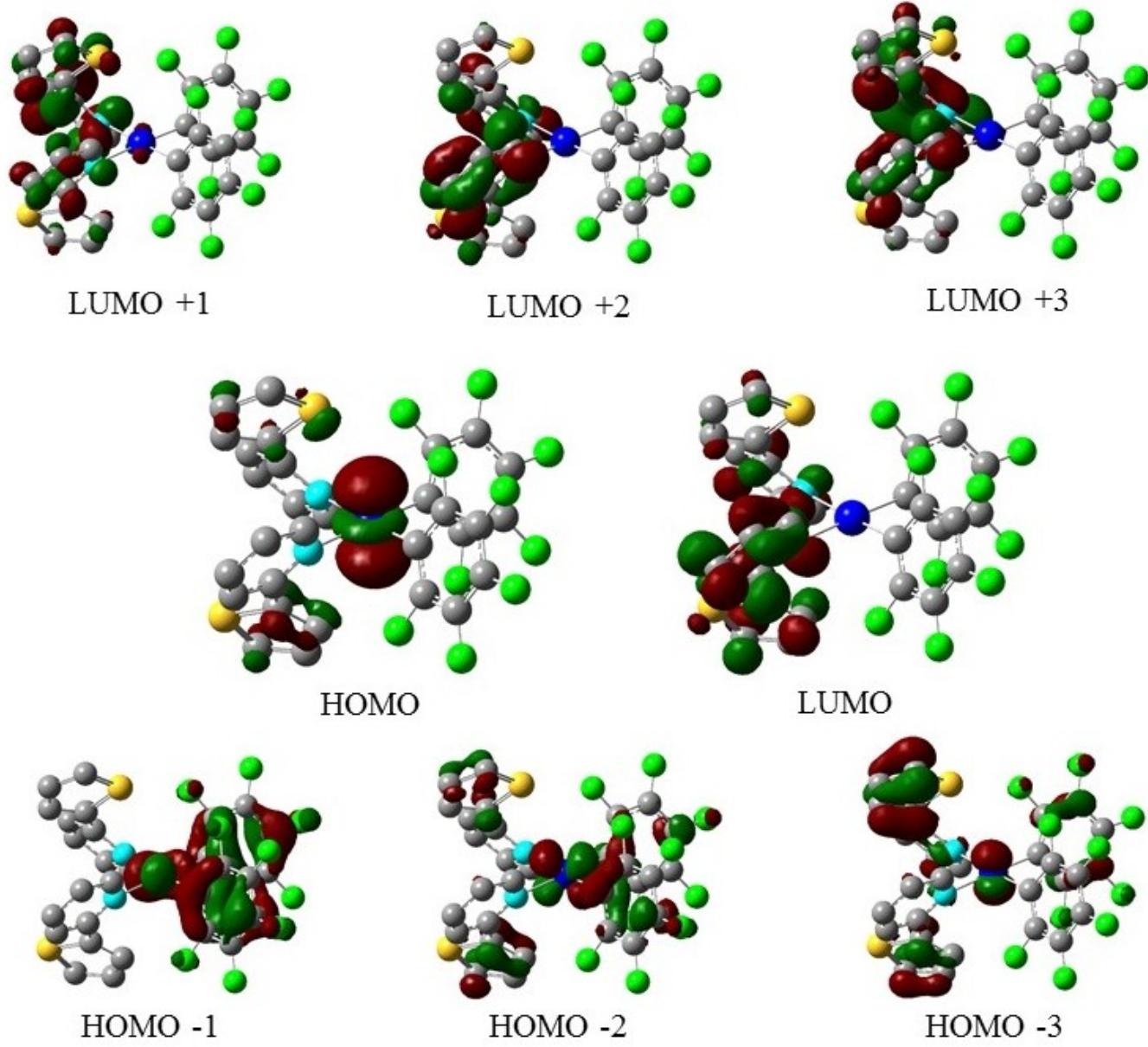
Fig. S17 Selected frontier Molecular Orbitals for complex **1a**.

LUMO +1   LUMO +2   LUMO +3

HOMO   LUMO

HOMO -1   HOMO -2   HOMO -3
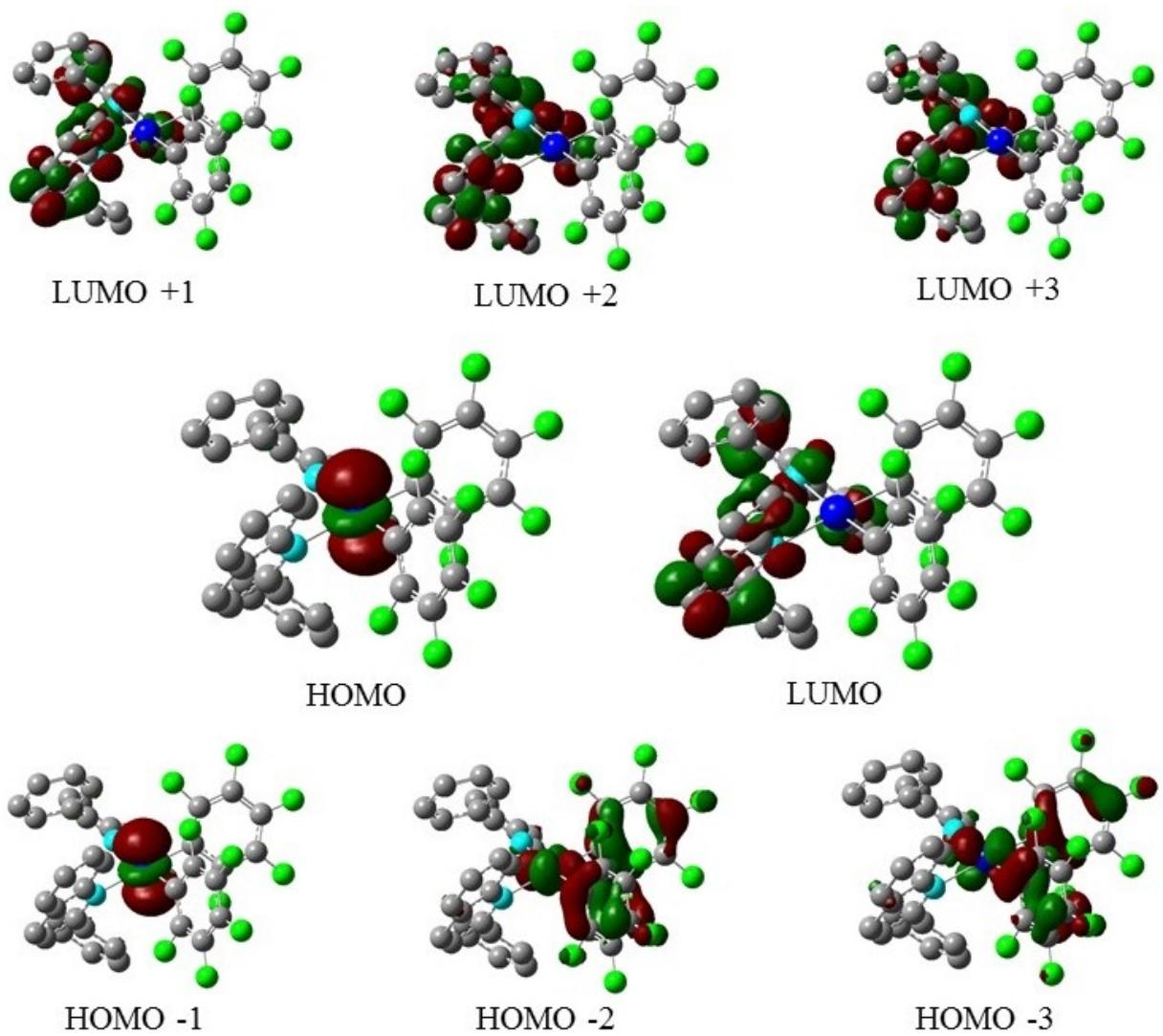
Fig. S18 Selected frontier Molecular Orbitals for complex **1c**.
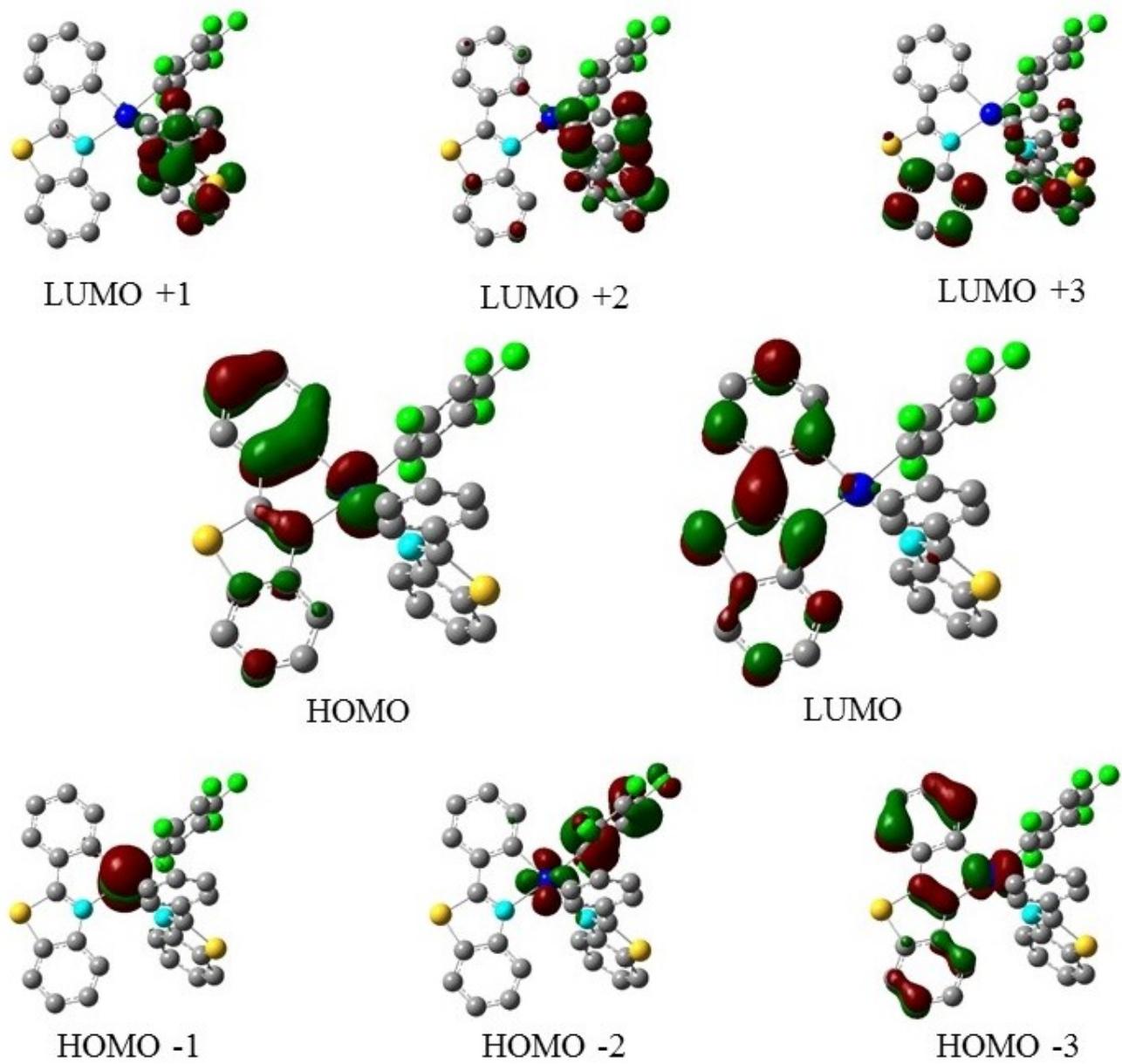
Fig. S19 Selected frontier Molecular Orbitals for complex **2b**.

LUMO +1

LUMO +2

LUMO +3

HOMO

LUMO

HOMO -1

HOMO -2

HOMO -3
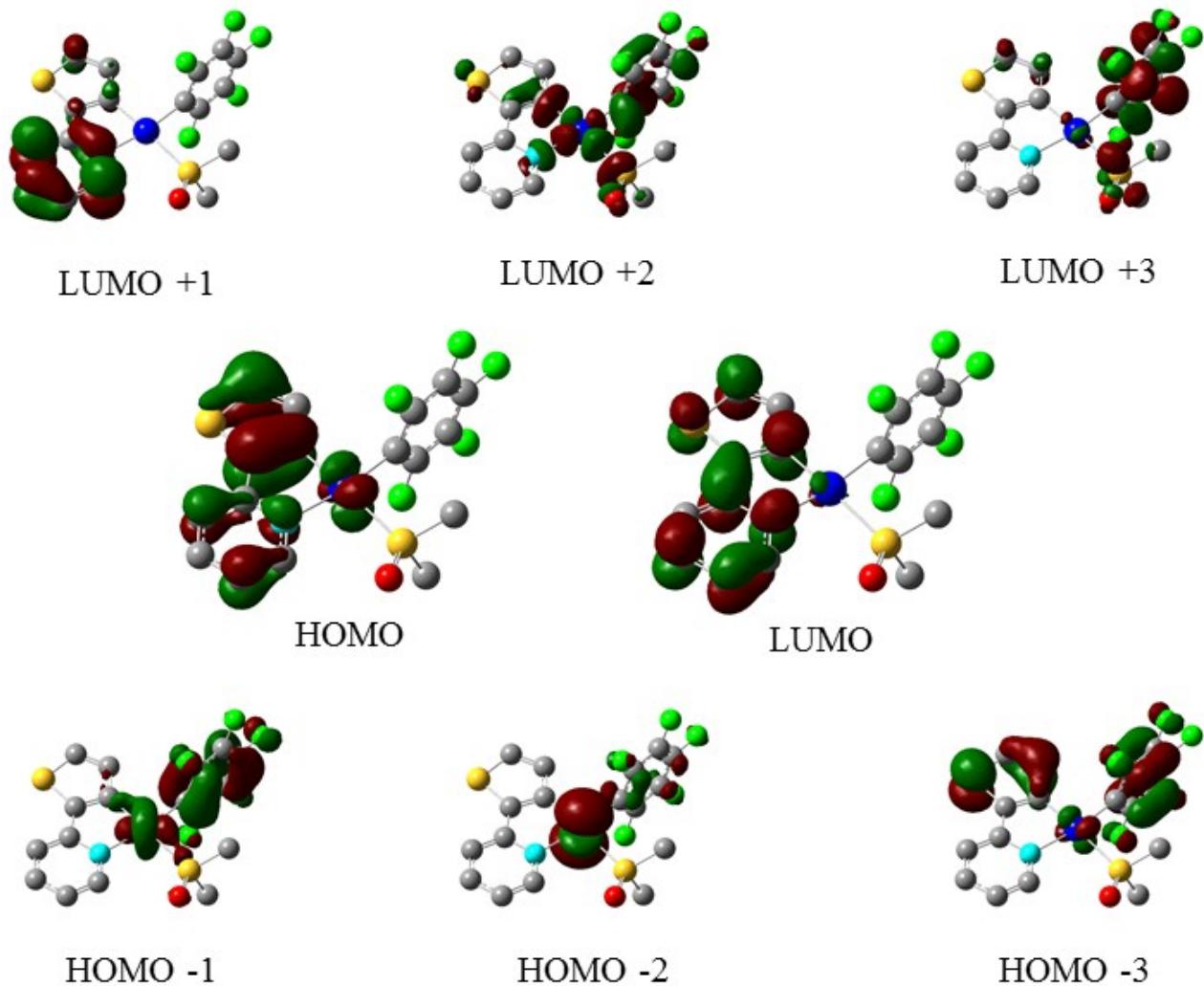
Fig. S20 Selected frontier Molecular Orbitals for complex **3a**.

Table S3 Selected vertical excitation energies singlets (S_0) and first triplets computed by TD-DFT/ SCRF (CH_2Cl_2) with the orbitals involved for complexes for **1a**, **1c**, **2b** and **3a**.

	State	λ_{ex}(calc)(nm)	f^a	Transition (% Contribution)
1a	T_1	435,93	0,0	H-6->LUMO (11%), H-2->LUMO (10%), HOMO->LUMO (27%)
	T_2	416,32	0,0	H-3->L+1 (21%), HOMO->L+1 (13%)
	S_1	374,76	0,0125	HOMO->LUMO (98%)
	S_2	367,86	0,0005	HOMO->L+1 (98%)
	S_3	339,32	0,0043	H-1->LUMO (97%)
	S_4	332,56	0,0105	H-1->L+1 (96%)
	S_5	322,96	0,0102	H-2->LUMO (92%)
	S_6	318,87	0,0256	H-2->L+1 (74%), HOMO->L+2 (13%)
	S_7	316,95	0,0081	H-2->L+1 (15%), HOMO->L+2 (79%)
	S_8	313,46	0,0021	HOMO->L+3 (42%), HOMO->L+4 (41%)
	S_9	308,42	0,1169	H-4->LUMO (11%), H-3->LUMO (74%)
	S_{10}	303,59	0,0496	H-4->L+1 (10%), H-3->L+1 (77%)
	S_{11}	300,08	0,0114	HOMO->L+3 (49%), HOMO->L+4 (38%)
1c	T_1	462,69	0,0	H-6->L+1 (18%), H-4->LUMO (28%), H-2->L+1 (1... H-1->LUMO (18%)
	T_2	461,09	0,0	H-6->LUMO (20%), H-4->L+1 (25%), H-2->LUMO... H-1->L+1 (16%)
	T_3	405,36	0,0	HOMO->LUMO (94%)
	S_1	400,50	0,0075	HOMO->LUMO (98%)
	S_2	388,44	0,0006	HOMO->L+1 (99%)
	S_3	365,57	0,0164	H-1->LUMO (95%)
	S_4	354,44	0,0414	H-2->LUMO (21%), H-1->L+1 (74%)
	S_5	350,28	0,0035	H-2->LUMO (74%), H-1->L+1 (21%)
	S_6	342,58	0,003	H-2->L+1 (93%)
	S_7	333,91	0,0563	H-4->LUMO (89%)
	S_8	322,70	0,0096	H-4->L+1 (16%), H-3->LUMO (76%)
	S_9	321,28	0,0413	H-4->L+1 (73%), H-3->LUMO (13%)
	S_{10}	318,04	0,0044	H-5->LUMO (47%), H-3->L+1 (50%)
	S_{11}	311,25	0,0152	HOMO->L+4 (85%)
	S_{12}	308,11	0,0058	H-7->LUMO (17%), H-6->LUMO (72%)
	S_{13}	306,96	0,0046	H-5->LUMO (46%), H-3->L+1 (45%)
2b	T_1	491,98	0,0	H-3->LUMO (11%), HOMO->LUMO (76%)
	T_2	419,99	0,0	H-6->L+1 (50%), H-1->L+1 (14%)
	S_1	394,56	0,099	HOMO->LUMO (84%)
	S_2	389,66	0,0208	H-1->LUMO (87%)
	S_3	379,23	0,0077	H-1->L+1 (48%), HOMO->L+1 (45%)
	S_4	374,07	0,0031	H-1->L+1 (46%), HOMO->L+1 (50%)
	S_5	351,52	0,0061	H-2->LUMO (93%)
	S_6	347,42	0,0161	H-2->L+1 (94%)
	S_7	330,68	0,1064	H-3->LUMO (78%)
	S_8	327,82	0,0124	H-3->L+1 (83%)

	S$_9$	316,70	0,002	H-4->L+1 (91%)
	S$_{10}$	312,08	0,0185	H-4->LUMO (86%)
	S$_{11}$	309,79	0,317	H-5->LUMO (76%)
	S$_{12}$	302,74	0,0264	H-5->L+1 (85%)
3a	T$_1$	527,81	0,0	HOMO->LUMO (90%)
	T$_2$	361,53	0,0	H-3->LUMO (17%), HOMO->L+1 (60%)
	S$_1$	374,06	0,1164	HOMO->LUMO (94%)
	S$_2$	337,60	0,0081	H-2->LUMO (11%), H-1->LUMO (89%)
	S$_3$	314,37	0,0052	H-2->LUMO (84%), H-1->LUMO (10%)
	S$_4$	304,447	0,0503	H-5->LUMO (21%), H-3->LUMO (21%), HOMO->L+1 (51%)
	S$_5$	298,407	0,1355	H-5->LUMO (14%), H-3->LUMO (69%), HOMO->L+1 (11%)
	S$_6$	295,56	0,0014	HOMO->L+2 (89%)
	S$_7$	290,13	0,0043	H-4->LUMO (94%)
	S$_8$	285,92	0,1805	H-5->LUMO (38%), H-1->L+2 (20%), HOMO->L+1 (27%)
	S$_9$	282,45	0,1241	H-5->LUMO (22%), H-2->L+2 (11%), H-1->L+2 (55%)

a) Oscillator Strength

Table S4 Composition (%) of frontier molecular orbitals in the first triple-state for **1a, 1c**, **2b** and **3a** in CH_2Cl_2

	1a					
	eV	$C_6F_5(1)$	$C_6F_5(2)$	Hthpy(1)	Hthpy(2)	Pt
SOMO	-3.83	0	0	1	98	1
SOMO-1	-5.99	4	5	14	4	74
	1c					
	eV	$C_6F_5(1)$	$C_6F_5(2)$	Hpq(1)	Hpq(2)	Pt
SOMO	-3.84	0	0	0	98	1
SOMO-1	-6.02	8	5	5	7	74
	2b					
	eV	C_6F_5	Hbt	bt	Pt	
SOMO	-3.64	0	0	95	5	
SOMO-1	-6.07	1	1	75	23	
	3a					
	eV	C_6F_5	thpy	dmso	Pt	
SOMO	-3.61	0	92	1	6	
SOMO-1	-6.24	0	78	1	20	
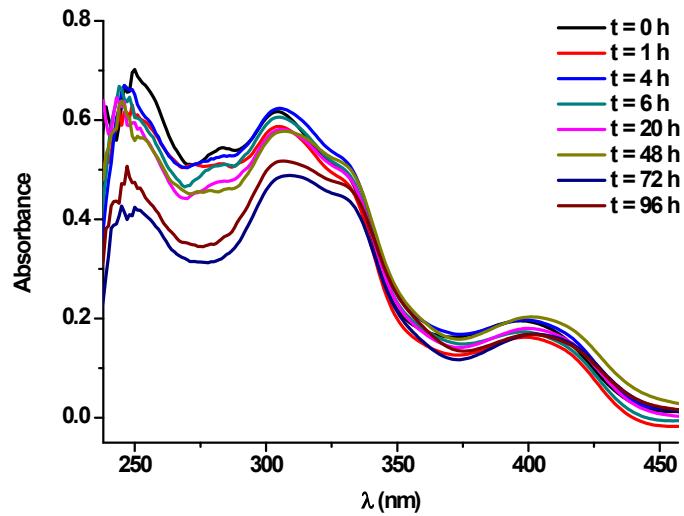
a)
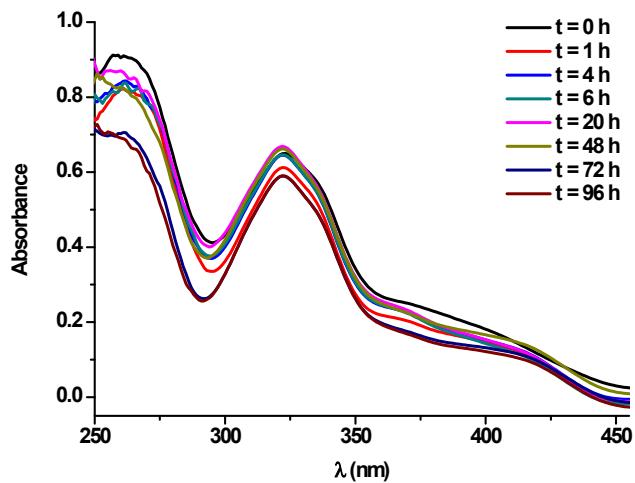
b)
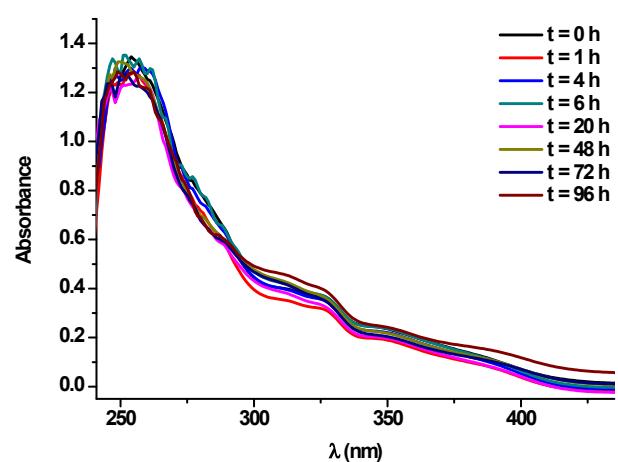
c)

Fig. S21 UV-vis absorption spectra of a) **3a**, b) **3b** and c) **4**, (5 x 10^{-5}M) recorded in DMSO (<1%)-cellular medium (see text) after been kept at room temperature since 0 h to 96 h (intervals in legends)
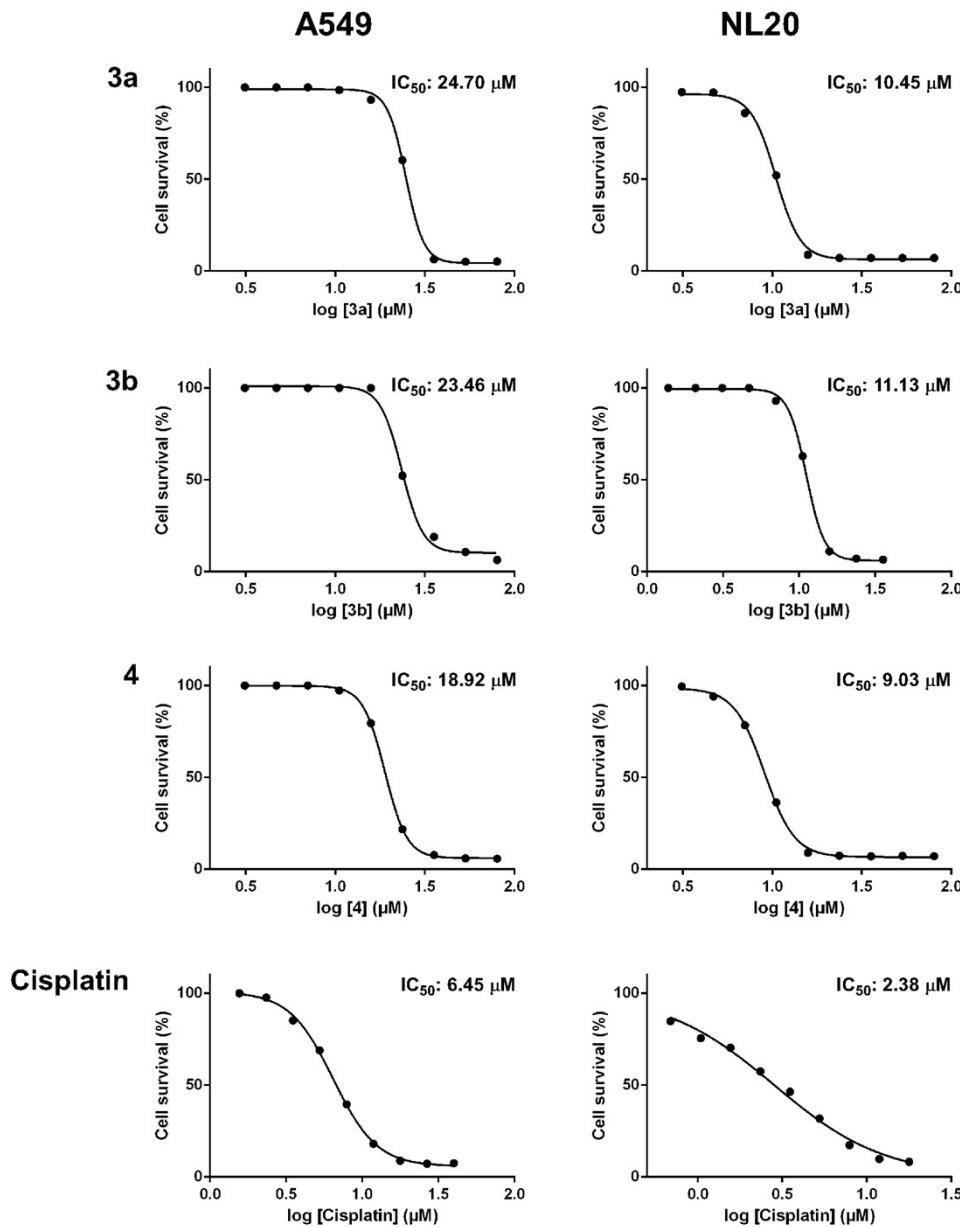
Fig. S22 Dose-response curves for determination of the IC_{50} cytotoxicity values of **3a**, **3b** and **4**, and their comparison with cisplatin, in A549 and NL20 cell lines. The IC_{50} values correspond to the dose required to inhibit 50% cellular growth, determined from the dose-dependence of surviving cells after cellular exposure to compounds for 72 h.
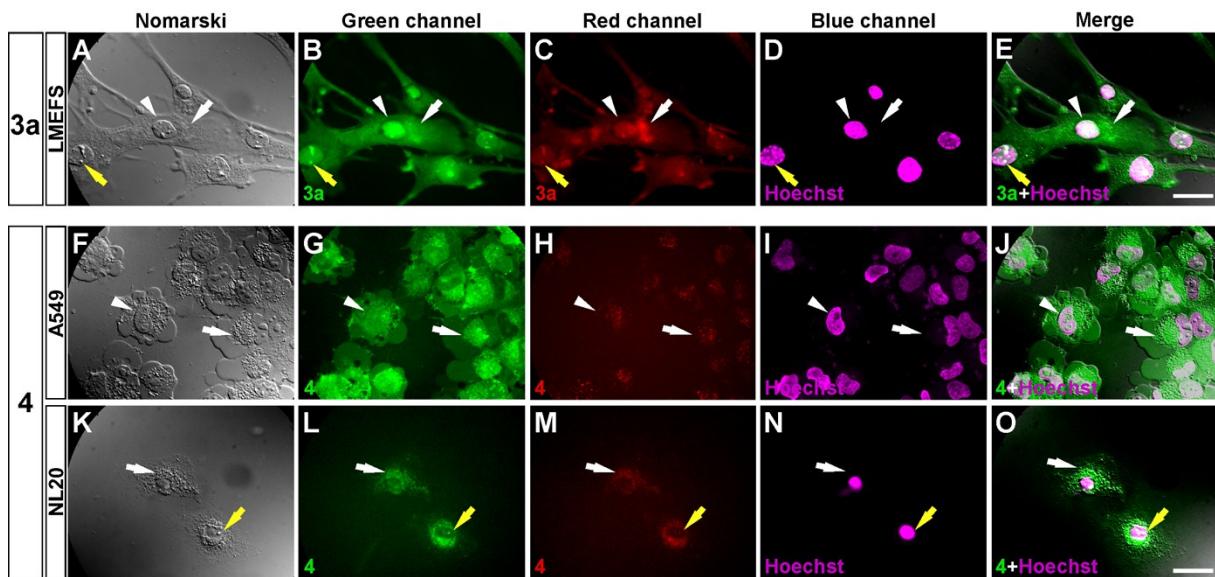
Fig. S23 Fluorescence images of mouse lung embryonic fibroblasts (LMEFs) treated with **3a,** and A549 and NL20 cells treated with complex **4.** Living LMEFs were treated with complex **3a** (A-E), and A549 and NL20 cells were treated with complex **4** (F-O) (both 40 μM), in combination with the DNA binder Hoechst 33258 (3.2 μM) for 30 min. Cells were visualized by microscopy either for Nomarski white-light transmission (A, E and K), or for fluorescence emission in green (B, G and L), red (C, H and M) and blue (D, I and N). Overlay of Nomarski, green, red and blue images are shown in right panels (E, J and O) (merged). Note that in LMFEs **3a** stains the cytoplasm, stronger in perinuclear areas (white arrows), nuclei (white arrowheads) and nucleoli (yellow arrows) in green, and in red with less intensity. Complex **4** stains the cytoplasm of A549 cells, stronger in the perinuclear structures (white arrows), and most nuclei (white arrowheads) including nucleoli, both in green, and in red (with less intensity). In NL20 cells, complex **4** stains the perinuclear cytoplasm (white arrows) and nucleoli (yellow arrows) in green, and in red with less intensity. Scales bar in E and O: 30 μm.
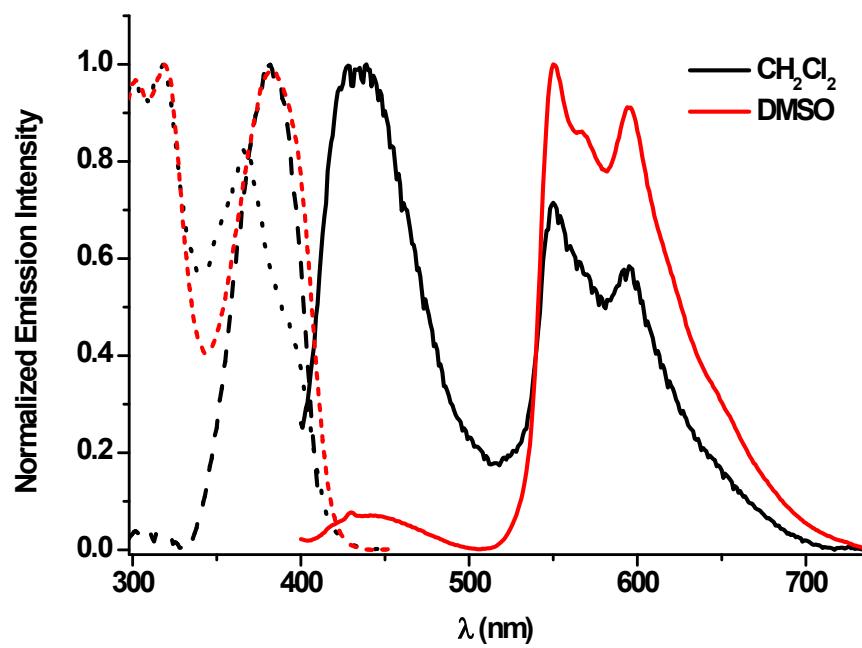
Fig. S24 Comparative normalized excitation and emission spectra of **3a** in CH$_2$Cl$_2$ and DMSO (5 x 10^{-5} M) at 298 K

Table S5 X-ray Crystallografic Data for **1a**, **1c**.0.75CH$_2$Cl$_2$, **2b**, **3a** and **3b**

	1a	1c.0.75CH$_2$Cl$_2$	2b	3a	3b
Empirical formula	C30 H14 F10 N2 Pt S2	C42 H22 F10 N2 Pt	C32 H17 F5 N2 Pt S2	C17 H12 F5 N O Pt S2	C21 H14 F5 N O Pt S2
F_w	851.64	939.70	783.68	600.49	650.54
T (K)	120(1)	173(1)	173(1)	173(1)	173 (1)
crystal system, space group	Orthorhombic, P bca	Monoclinic, P 21/n	Monoclinic, P 21/a	Triclinic, P -1	Triclinic, P -1
a(Å)	12.6350(2)	8.2453(2)	14.9033(5)	6.7971(2)	7.5475(2)
b(Å)	18.4730(3)	26.5307(7)	12.3384(4)	10.3253(5)	11.4335(5)
c(Å)	23.9410(3)	16.6300(4)	15.0986(4)	12.4185(6)	11.8516(5)
α(deg)	90	90	90.	84.911(2)	99.861(2)
β(deg)	90	94.703(2)	105.414(2)	85.894(3)	98.362(2)
γ(deg)	90	90	90.	88.980(3)	91.328(3)
volume (A^3)	5587.98(14)	3625.62(16)	1129.94(9)	865.84(6)	995.69(7)
Z	8	4	4	2	2
D_{calcd} (Mg/m^3)	2.025 Mg/m^3	1.722	1.945	2.303	2.170
absorption coefficient (mm^{-1})	5.264	3.955	5.461	8.403	7.316
F(000)	3264	1824	1512	568	620
θ range for data collection (deg)	3.37 to 25.68	1.449 to 25.026	3.258 to 27.476	1.650 to 24.711	3.470 to 24.707
no of data / restraints / params	5299 / 0 / 358	6376 / 0 / 496	6068 / 0 / 379	2795 / 0 / 215	3284 / 0 / 280
goodness-of-fit on F$^{2[a]}$	1.037	1.128	1.096	1.197	0.938
final R indices [I>2σ(I)][a]	R1 = 0.0260, wR2 = 0.0543	R1 = 0.0445, wR2 = 0.1169	R1 = 0.0262, wR2 = 0.0551	R1 = 0.0547, wR2 = 0.1467	R1 = 0.0345, wR2 = 0.0932
R indices (all data)[a]	R1 = 0.0340, wR2 = 0.0583	R1 = 0.0551, wR2 = 0.1250	R1 = 0.0317, wR2 = 0.0571	R1 = 0.0556, wR2 = 0.1501	R1 = 0.0349, wR2 = 0.0939
largest diff peak and hole (e.Å^{-3})	2.328 and -1.255	2.131 and -2.136	1.417 and -0.779	2.834 and -3.185	1.768 and -2.827

[a] $R1 = \Sigma(|F_o| - |F_c|)/\Sigma|F_o|$; w$R2 = [\Sigma w(F_o^2 - F_c^2)^2/\Sigma wF_o^2]^{1/2}$; goodness of fit = $\{\Sigma[w(F_o^2 - F_c^2)^2]/(N_{obs} - N_{param})\}^{1/2}$; $w = [\sigma^2(F_o) + (g_1 P)^2 + g_2 P]^{-1}$; $P = [\max(F_o^2; 0 + 2F_c^2]/3$.

Complete reference 39:

Gaussian 09, Revision B.01, M. J. Frisch, G. W. Trucks, H. B. Schlegel, G. E. Scuseria, M. A. Robb, J. R. Cheeseman, G. Scalmani, V. Barone, B. Mennucci, G. A. Petersson, H. Nakatsuji, M. Caricato, X. Li, H. P. Hratchian, A. F. Izmaylov, J. Bloino, G. Zheng, J. L. Sonnenberg, M. Hada, M. Ehara, K. Toyota, R. Fukuda, J. Hasegawa, M. Ishida, T. Nakajima, Y. Honda, O. Kitao, H. Nakai, T. Vreven, J. A. Montgomery, Jr., J. E. Peralta, F. Ogliaro, M. Bearpark, J. J. Heyd, E. Brothers, K. N. Kudin, V. N. Staroverov, T. Keith, R. Kobayashi, J. Normand, K. Raghavachari, A. Rendell, J. C. Burant, S. S. Iyengar, J. Tomasi, M. Cossi, N. Rega, J. M. Millam, M. Klene, J. E. Knox, J. B. Cross, V. Bakken, C. Adamo, J. Jaramillo, R. Gomperts, R. E. Stratmann, O. Yazyev, A. J. Austin, R. Cammi, C. Pomelli, J. W. Ochterski, R. L. Martin, K. Morokuma, V. G. Zakrzewski, G. A. Voth, P. Salvador, J. J. Dannenberg, S. Dapprich, A. D. Daniels, O. Farkas, J. B. Foresman, J. V. Ortiz, J. Cioslowski, and D. J. Fox, Gaussian, Inc., Wallingford CT, 2010.